Supplementary Material (ESI) for PCCP

Theoretical Study of the Temperature Dependence of Dynamic Effects in Thymidylate Synthase

Electronic Supplementary Information

Natalia Kanaan, Maite Roca, Iñaki Tuñón, Sergio Martí,* Vicent Moliner.*

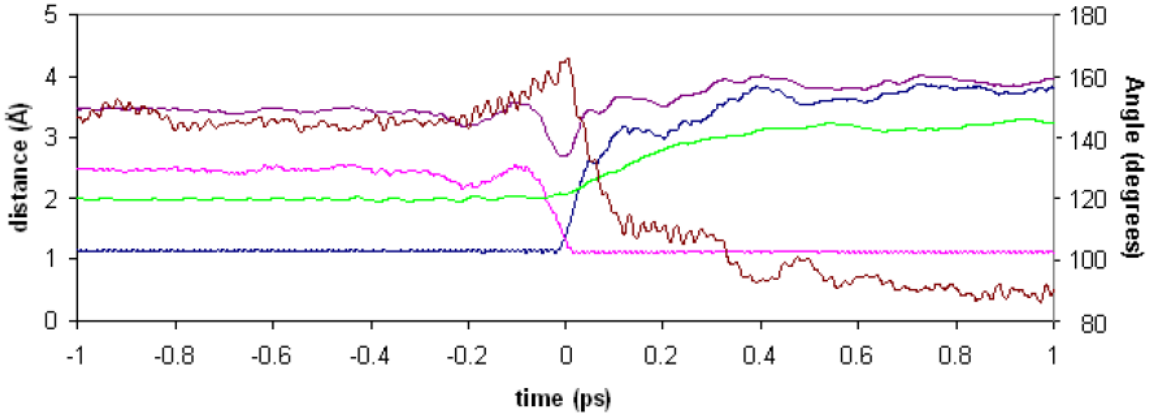

Figure S1. Time evolution of key distances and angle defining the chemical reaction, for reactive trajectories at 278 K. Distance C8-C7 (purple line), C8-Ht (blue line), Ht-C7 (magenta line), C6-S (green line) and the C8-Ht-C7 angle (brown line).

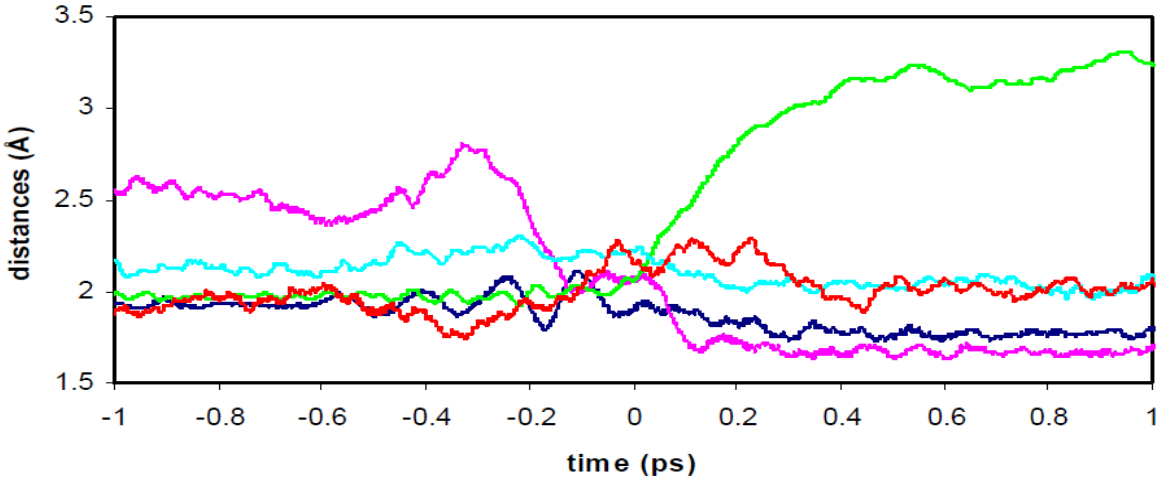

Figure S2. Time evolution of key distances established with residues of the active site for reactive trajectories at 278 K: S-Wat40 distance (dark blue line), S-Arg166 distance (magenta line), O3P-Arg166 distance (red line), O2-Asp169 distance (light blue line) and C6-S distance (green line).

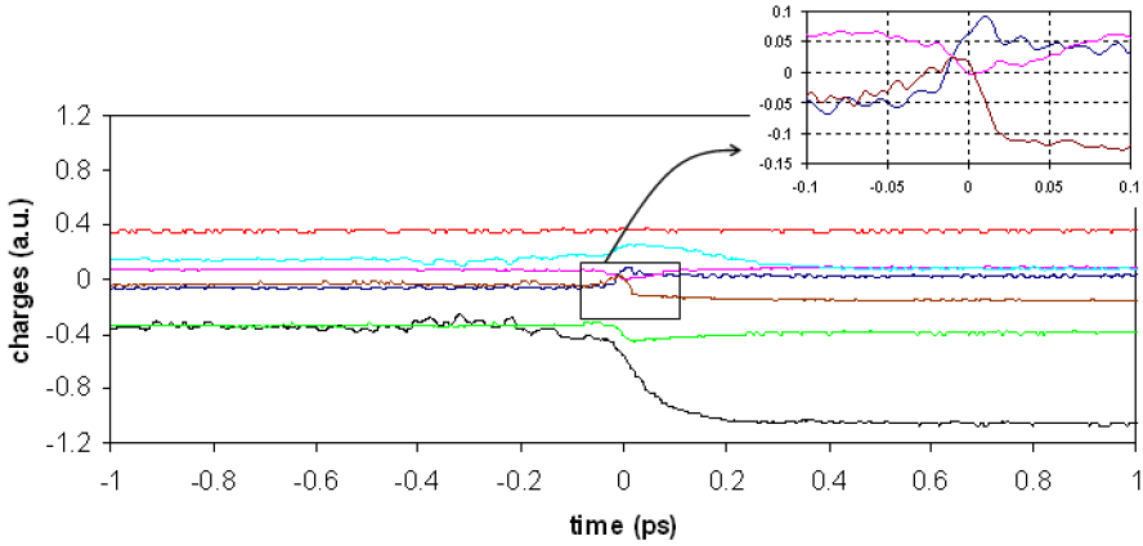

Figure S3. Time evolution of Mulliken charges of key atoms averaged for reactive trajectories at 278 K: C8 (dark blue line), Ht (magenta line), C7 (brown line), C6 (light blue line), S (black line), O4 (green line) and C4 (red line).

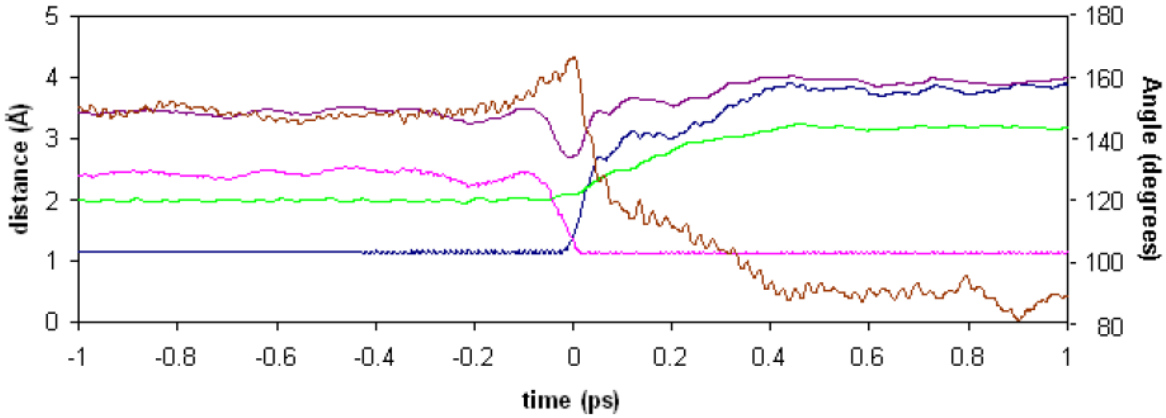

Figure S4. Time evolution of key distances and angle defining the chemical reaction, for reactive trajectories at 303 K. Distance C8-C7 (purple line), C8-Ht (blue line), Ht-C7 (magenta line), C6-S (green line) and the C8-Ht-C7 angle (brown line).

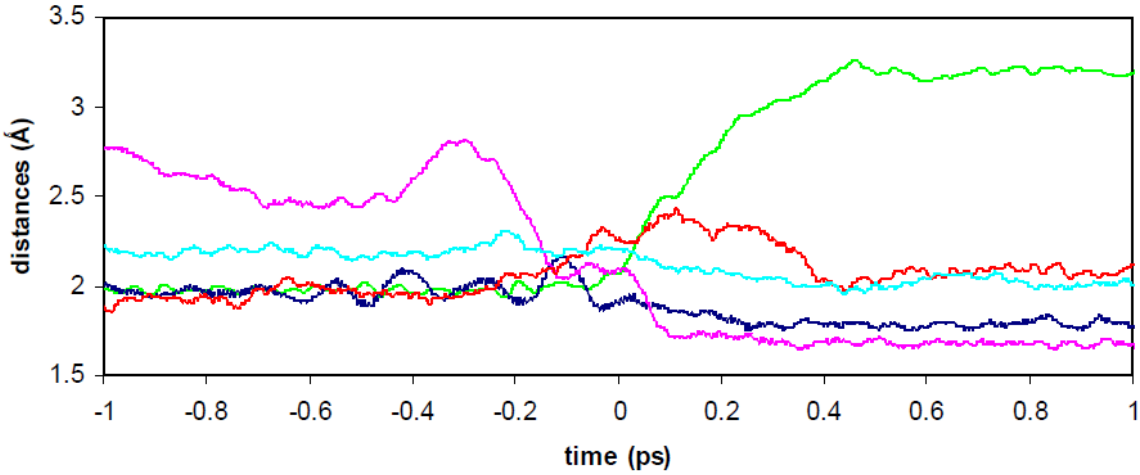

Figure S5. Time evolution of key distances established with residues of the active site for reactive trajectories at 303 K: S-Wat40 distance (dark blue line), S-Arg166 distance (magenta line), O3P-Arg166 distance (red line), O2-Asp169 distance (light blue line) and C6-S distance (green line).

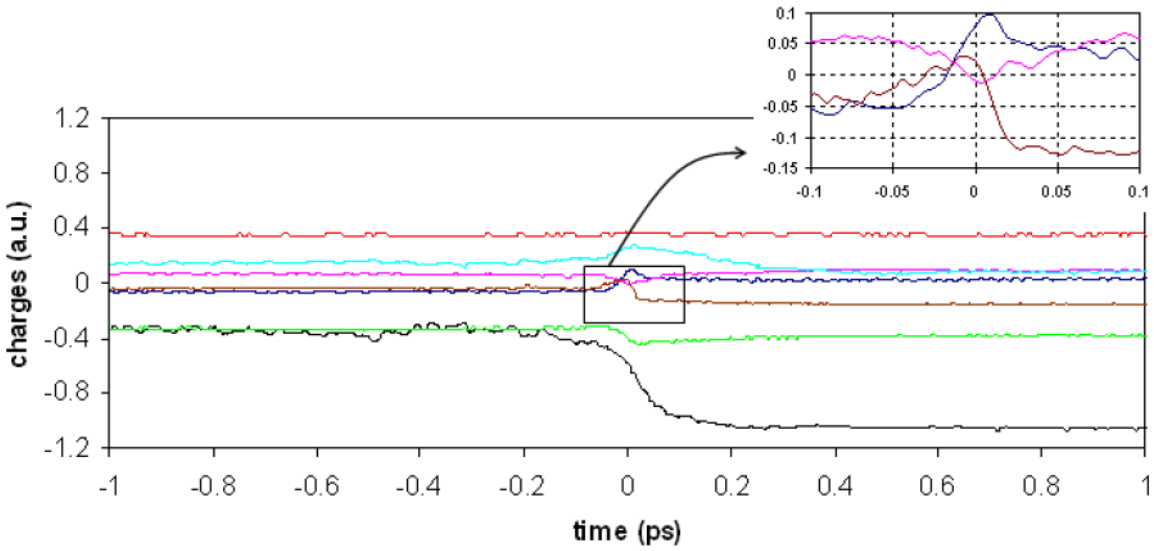

Figure S6. Time evolution of Mulliken charges of key atoms averaged for reactive trajectories at 303 K: C8 (dark blue line), Ht (magenta line), C7 (brown line), C6 (light blue line), S (black line), O4 (green line) and C4 (red line).

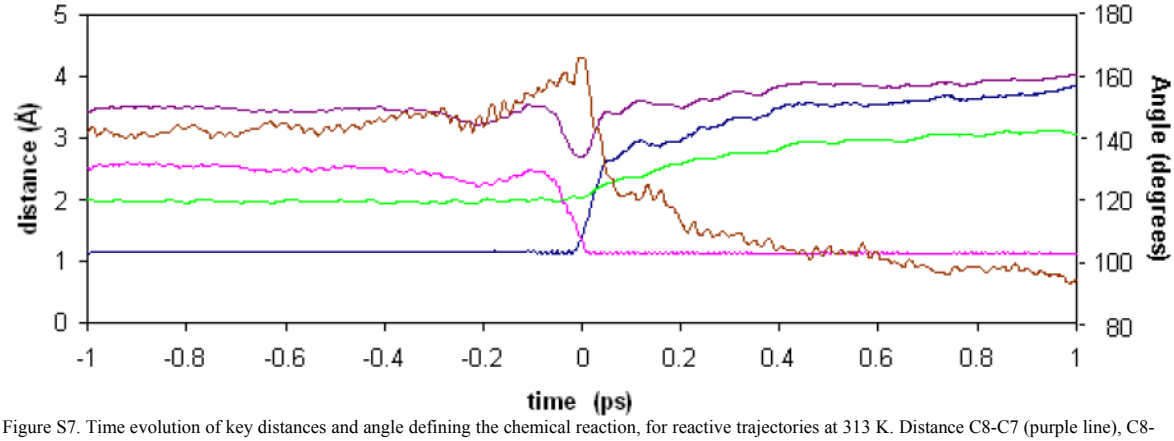

Figure S7. Time evolution of key distances and angle defining the chemical reaction, for reactive trajectories at 313 K. Distance C8-C7 (purple line), C8-Ht (blue line), Ht-C7 (magenta line), C6-S (green line) and the C8-Ht-C7 angle (brown line).

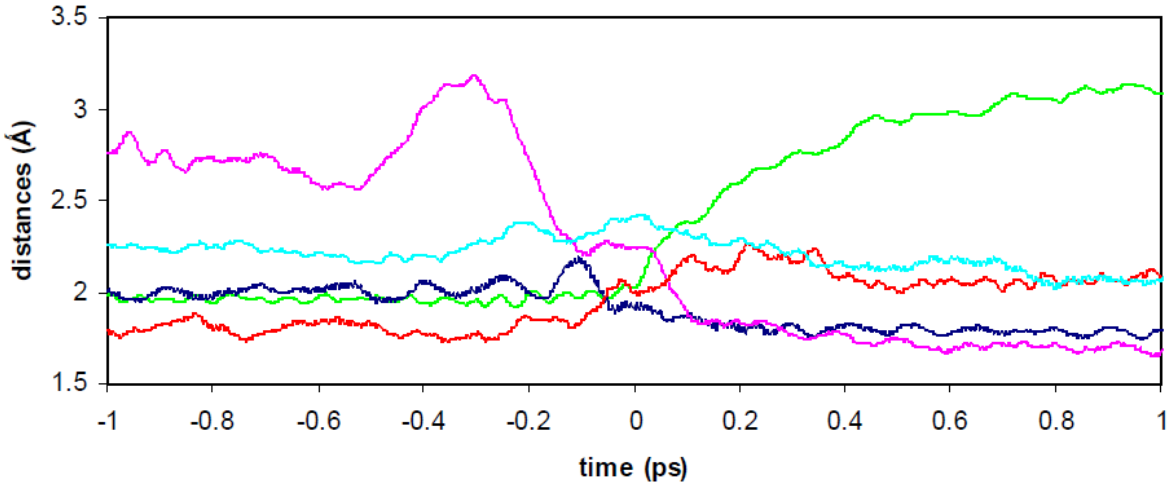

Figure S8. Time evolution of key distances established with residues of the active site for reactive trajectories at 313 K: S-Wat40 distance (dark blue line), S-Arg166 distance (magenta line), O3P-Arg166 distance (red line), O2-Asp169 distance (light blue line) and C6-S distance (green line).

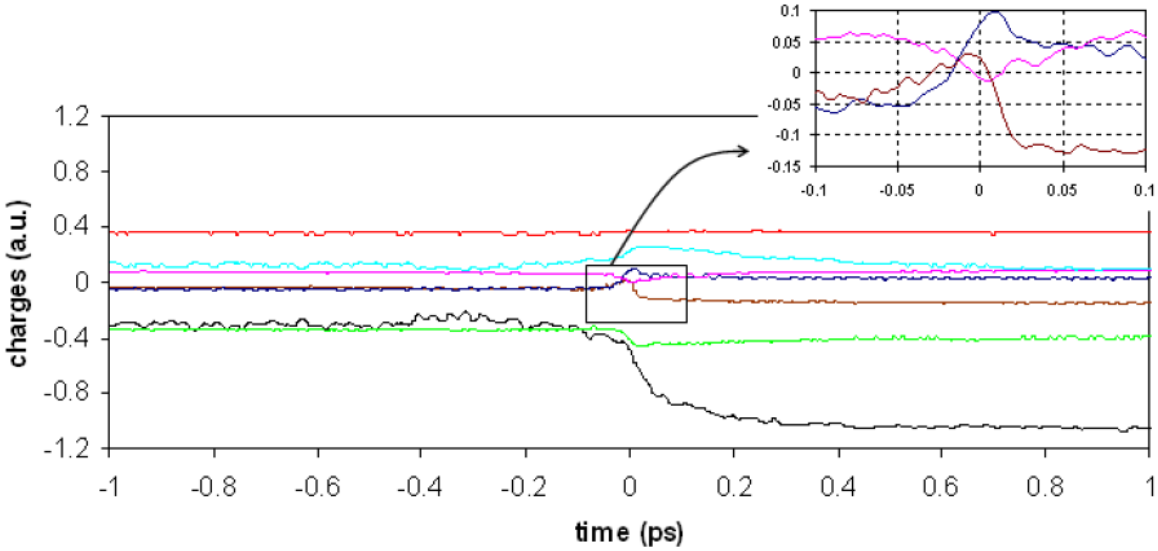

Figure S9. Time evolution of Mulliken charges of key atoms averaged for reactive trajectories at 313 K: C8 (dark blue line), Ht (magenta line), C7 (brown line), C6 (light blue line), S (black line), O4 (green line) and C4 (red line).

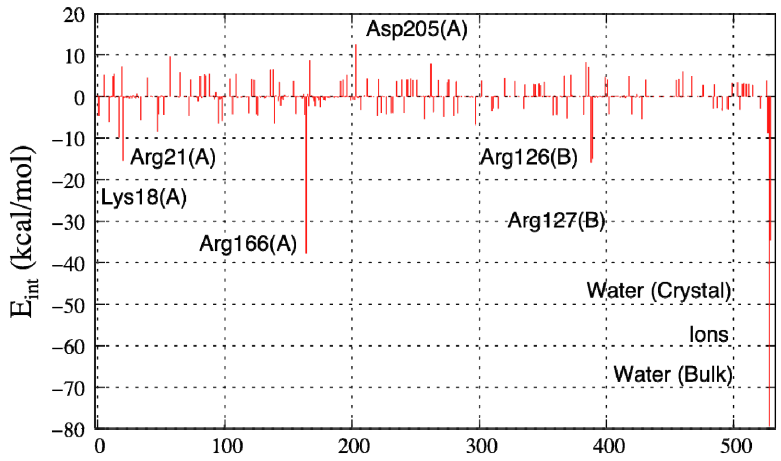

Figure S10. Contributions of individual amino acid residues to interaction electrostatic energies (in kcal/mol) computed at AM1/MM level from averaged represetative structures of the transition state. The most important interactions are assigned.

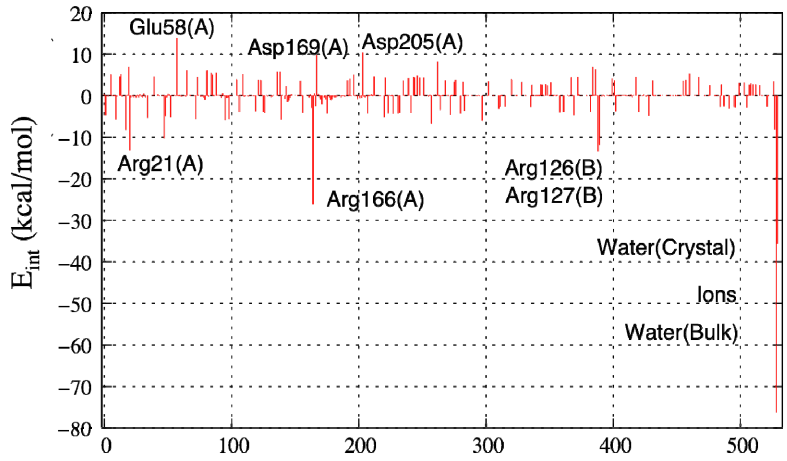

Figure S11. Contributions of individual amino acid residues to interaction electrostatic energies (in kcal/mol) computed at B3LYP/6-31g(d,p)/MM level from averaged represetative structures of the transition state. The most important interactions are assigned.

Table S1. Weights of the coordinates (together with their standard deviations) of the key atoms in the transition vectors obtained using two different sizes of the Hessians (see text). Values have been averaged over 12 different transition structures. Cys146, Folate and dUMP accounts for the rest of the atoms of these residues. Results are reported for 278 K.

	Small Hessian	Large Hessian
C8	0.218 ± 0.017	0.258 ± 0.016
Ht	0.436 ± 0.005	0.440 ± 0.005
C7	0.246 ± 0.018	0.214 ± 0.016
N9	0.009 ± 0.005	0.007 ± 0.03
C6	0.0134 ± 0.0014	0.0079 ± 0.0010
S	0.0089 ± 0.0011	0.0037 ± 0.0007
C5	0.0168 ± 0.0012	0.0147 ± 0.0013
H71	0.0078 ± 0.0008	0.0091 ± 0.0010
H72	0.0133 ± 0.0018	0.0135 ± 0.0019
Cys146	0.0017 ± 0.0021	0.0011 ± 0.0013
Folate	0.029 ± 0.007	0.027 ± 0.006
dUMP	0.0095 ± 0.0010	0.0111 ± 0.0009
Arg166	-	0.00053 ± 0.00014
WAT40	-	0.00054 ± 0.00007

Table S2. Weights of the coordinates (together with their standard deviations) of the key atoms in the transition vectors obtained using two different sizes of the Hessians (see text). Values have been averaged over 12 different transition structures. Cys146, Folate and dUMP accounts for the rest of the atoms of these residues. Results are reported for 303 K.

	Small Hessian	Large Hessian
C8	0.217 ± 0.017	0.260 ± 0.017
Ht	0.434 ± 0.006	0.440 ± 0.004
C7	0.245 ± 0.015	0.210 ± 0.014
N9	0.012 ± 0.007	0.008 ± 0.04
C6	0.0140 ± 0.0013	0.0085 ± 0.0014
S	0.0095 ± 0.0012	0.0040 ± 0.0010
C5	0.0163 ± 0.0010	0.0138 ± 0.0010
H71	0.0072 ± 0.0010	0.0089 ± 0.0011
H72	0.0133 ± 0.0014	0.0130 ± 0.0012
Cys146	0.002 ± 0.003	0.0014 ± 0.0018
Folate	0.033 ± 0.009	0.029 ± 0.006
dUMP	0.0091 ± 0.0011	0.0108 ± 0.0011
Arg166	-	0.00056 ± 0.00023
WAT40	-	0.00051 ± 0.00006

Table S3. Weights of the coordinates (together with their standard deviations) of the key atoms in the transition vectors obtained using two different sizes of the Hessians (see text). Values have been averaged over 12 different transition structures. Cys146, Folate and dUMP accounts for the rest of the atoms of these residues. Results are reported for 313 K.

	Small Hessian	Large Hessian
C8	0.240 ± 0.019	0.276 ± 0.018
Ht	0.442 ± 0.010	0.444 ± 0.009
C7	0.220 ± 0.016	0.192 ± 0.014
N9	0.010 ± 0.005	0.008 ± 0.004
C6	0.0118 ± 0.0008	0.0072 ± 0.0007
S	0.0076 ± 0.0008	0.0030 ± 0.0005
C5	0.01424 ± 0.0013	0.0127 ± 0.0013
H71	0.0071 ± 0.0018	0.0086 ± 0.0019
H72	0.0148 ± 0.0020	0.0147 ± 0.0012
Cys146	0.0021 ± 0.0015	0.0016 ± 0.0017
Folate	0.031 ± 0.009	0.029 ± 0.008
dUMP	0.0097 ± 0.0009	0.0113 ± 0.0009
Arg166	-	0.00045 ± 0.00014
WAT40	-	0.00052 ± 0.00008